CHAPTER 232

Modelling Sand Transport and Profile Evolution on Macrotidal Beaches

Paul.R.Fisher[1] & Tim.J.O'Hare[2]

Abstract

An empirical model is presented which simulates the effect of tidal translation of cross-shore sediment flux patterns, in support of a hypothesis that wave height *and* tidal range are the key influences in the formation of characteristic macrotidal beach profiles. The energetics-based model is based upon field observations of cross shore currents and sediment fluxes from three high-energy macrotidal (tide range>4m) locations around the U.K, chosen as representations of dissipative, intermediate and reflective environments (after Wright and Short, 1984). The observed depth-dependant flux patterns are translated across linear beach profiles, with gradients modelled from sediment characteristics (Dean 1977, Kriebel et al 1991), the evolution of characteristic macrotidal beach profiles and the development of attendant features such as break-point bars, low tide terraces, and steepened foreshores are observed.

Introduction

The morphological significance of tidal translation of the swash, surf and shoaling wave zones across the beachface has received increasing attention over the last fifteen years (Wright et al (1982), Short (1991), Masselink (1993), Masselink and Short (1993)). It has been suggested that the continual variation in water depth by the tidal signal in a *macrotidal* environment is responsible for temporal variations in local dynamics. Furthermore, the intermittence of swash and surf processes in the high-tidal zone modifies the dynamics of that zone, whereas the mid and low-tidal zone dynamics are more similar to nearshore and offshore zones on micro-tidal beaches (Wright et al, 1982).

This contribution sets out to give some insight into the effects of asymmetric residence times of the water level on the beachface within macrotidal regimes.

[1]Research student, [2]Senior Lecturer, Institute of Marine Studies, University of Plymouth, Drake Circus, Plymouth, Devon, UK, PL4 8AA

According to the classification of Bird (1969) macrotidal regimes are those locations where the mean maximum tidal range during a month is greater than 4 metres, mesotidal regimes experience a mean maximum tidal range between 2 and 4 metres, and microtidal regimes are between 1 and 2 metres. While much work has been done relating the effects of a varying wave field on sediment transport processes in macrotidal regimes, (e.g. Wright et al (1982), Wright and Short (1984)), it is not clear how transport processes are modulated by a continual rise and fall of the water level by the tidal signal. This effect is pronounced within macrotidal environments where migration velocities and widths of swash, surf and wave shoaling zones are variant during the tidal cycle dependant on(a) the phase of

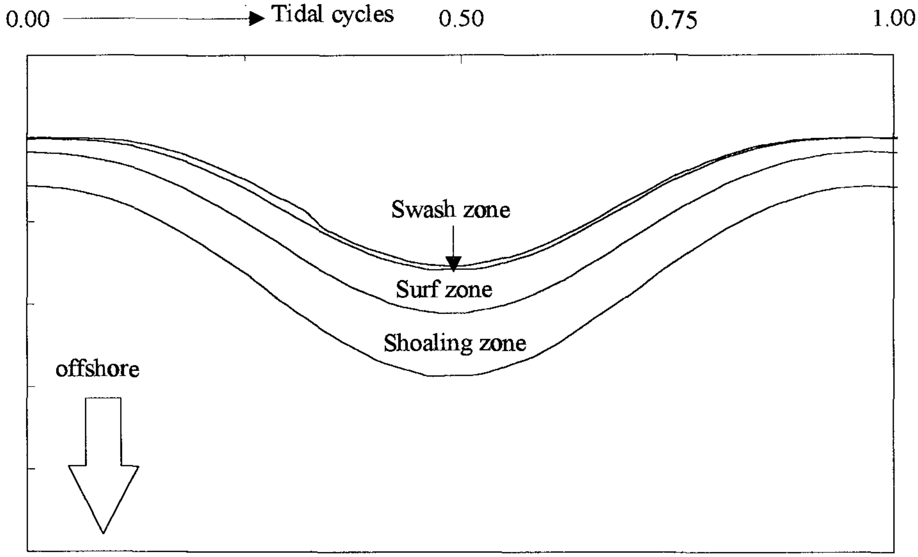

Figure 1. Tidal translation of swash, surf and shoaling zone processes across a beachface of exponential form. Because of the shoreward increasing beach gradient swash, surf and shoaling zones narrow significantly at high tide levels.

the tide and (b) the local gradient of the beach. The tidal variation in magnitude and position of these zones is illustrated in Figure 1 for the case of an exponential beachface. The approach taken in this study is to oscillate simple empirical models of cross-shore sediment transport across a beachface, allowing the profile to respond to the resulting patterns of erosion and deposition. The empirical model used is constructed from field observations of water and sediment dynamics at a variety of high energy macrotidal locations around the U.K during the British Beach and Nearshore Dynamics (B-BAND) experiment.

A useful overview of the B-BAND experiment is given by Davidson et al (1993). This three-year experiment investigated surf zone processes at three high energy macrotidal locations around the UK. The sites were chosen to represent dissipative, intermediate and reflective beaches following the morphodynamic classifications of Wright and Short (1984). The locations are illustrated in Figure 2 along with typical beach profiles and are described briefly in turn.

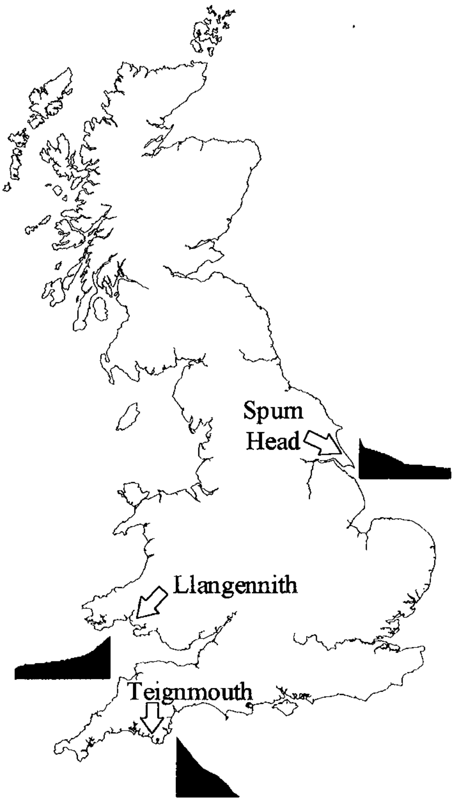

Llangennith: A dissipative high energy beach with a shallow beach gradient (0.014-0.020) with fine to medium quartz sands (D_{50}=0.21mm). This beach is west facing, has a tide range up to 9 metres, and broad surf (up to 350m) and intertidal (~ 500m) zones.

Spurn Head: An intermediate beach located near the end of a 5km long spit facing the North Sea. The beach profile comprises a steep high tide beach ($\tan\beta \sim 0.0975$) and a low tide terrace ($\tan\beta \sim 0.023$, and D_{50}=0.35mm). This beach has a tide range up to 6m and experiences strong longshore tidal currents which have a significant effect on surf zone dynamics.

Teignmouth: A reflective beach site facing south-east into the English Channel sheltered from Atlantic swell. The beach is backed by a sea wall, and has a gradient of 0.067-0.142. Cross - shore variation of sediment size at this location is significant, with a D_{50} value of 0.24mm. Tidal range is 6 metres.

Figure 2. Location of B-BAND field sites around the UK, showing typical cross-sectional profiles.

Shape Function Approach To Sediment Transport

Foote (1994), Foote et al (1994), and Russell and Huntley (1996) examined field measurements of cross-shore sediment transport from these three locations. They calculated velocity moment contributions to sand transport, by assuming the instantaneous velocity field to be composed of the following contributions:

$$u = \bar{u} + u_S + u_L \tag{1}$$

where $\bar{u}$ is the mean flow, u_S is the incident wave component of velocity, and u_L is the long wave component. Using Bagnold's (1963, 1966) uni-directional stream flow total load sediment transport model, modified by Bailard (1981, 1987) for cross shore sediment transport under bi-directional flow, Guza and Thornton (1985) used field measurements to examine the relative importance of the velocity moment terms in Bailards model, and found the transport significant terms to be (in normalised form):

$$\overline{|u|^2 u} \Big/ \left(\overline{u^2}\right)^{3/2} \qquad \text{for bedload transport, and} \qquad (2)$$

$$\overline{|u|^3 u} \Big/ \left(\overline{u^2}\right)^{2} \qquad \text{for suspended load transport} \qquad (3)$$

Foote et al (1994) examined the cross-shore distribution of the significant moments for bedload and suspended load and found in both cases that the sum predicted a net onshore movement shoreward of the breakpoint and a net offshore movement seaward of the breakpoint. To clarify this pattern for each case they normalised the water depth by the depth of wave breaking. The position of wave breaking was determined from the position of maximum wave height from pressure transducer records and this was checked with visual observations in the field. Combining data from all three field sites they noted that not only was there a pattern of net onshore transport shoreward of wave breaking and a net offshore transport seaward of it, but that a curve could be reasonably fitted through the velocity moments calculated for the interim positions.

They subsequently proposed the existence of quasi-universal, cross-shore sediment transport spatial distribution curves for bed load and suspended load on high energy beaches. These sediment 'shape functions' are illustrated in Figure 3. Third order polynomials are fitted through each data set, with one root at x=0, y=0 (zero transport at the shoreline). O'Hare (1994) proposed that this 'shape function' approach be adopted to develop a tentative cross-shore sediment transport model, suggesting that the patterns observed in the B-BAND data are in fact required by the break-point bar hypothesis, and that characteristic macrotidal profiles may be constructed by the repeated tidal excursion of the shape function. This contribution presents the preliminary results from the development of such a model.

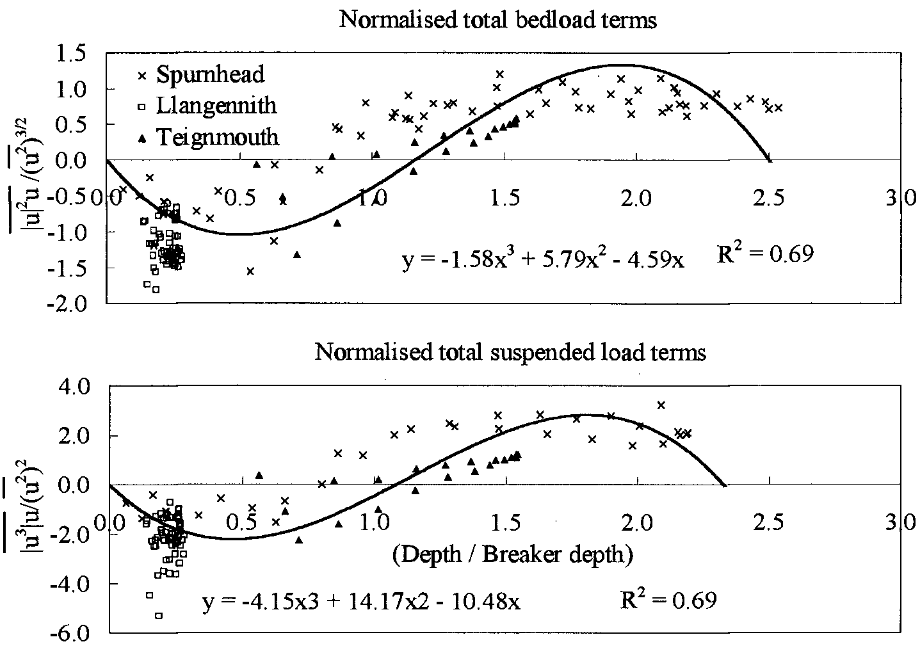

Figure 3. Sediment transport shape functions obtained from the B-BAND data.

Model Description

The simulation model migrates the proposed shape functions for bed and suspended load across a beachface. The input parameters for the model are breaker height H_b, grain diameter ϕ, tide range, wave period T, sediment and fluid densities ρ_s and ρ, gravity, kinematic fluid viscosity υ, bed drag coefficient C_d, and bed and suspended load efficiencies ε_b and ε_s. Related parameters such as sediment repose angle, $\tan\phi$, and sediment porosity, n, are evaluated using an empirical model (Allen, 1970).

The first stage for the simulation model is to evaluate the grain buoyancy and fall velocity of the beach sediment according to the CERC Shore Protection Manual procedures (US Army Corps of Coastal Engineers, 1984):

Grain buoyancy (A): $$\frac{(\rho_s - \rho)}{\rho}\frac{gD^3}{\upsilon^2} \qquad (4)$$

Sediment fall velocity (w):

$$w = \frac{1}{18}\frac{(\rho_s - \rho)}{\rho}\frac{gD^2}{\upsilon} \quad \text{(for A<39)} \qquad \frac{\left\{\frac{(\rho_s - \rho)g}{\rho}\right\}^{0.7} \cdot D^{1.1}}{6\upsilon^{0.4}} \quad \text{(for } 39<A<10^4\text{)} \qquad \left\{\frac{(\rho_s - \rho)gD}{0.91\rho}\right\}^{0.5} \quad \text{(for } A>10^4\text{)} \tag{5}$$

Breaking depth is then calculated iteratively according to the model of Le Mehaute (1961) using an initial estimated value for breaking depth (taken as 5m):

$$d_b = \left[\frac{H_b\left(gd_bT^2\right)^{0.5} gT^2}{0.12\tanh 2\pi d_b}\right] \tag{6}$$

Next breaker coefficient (γ) and breaking wavelength (L_b) are evaluated from:

$$\gamma = \frac{H_b}{d_b} \qquad \text{(from Galvin, 1972)} \tag{7}$$

$$L_b = \sqrt{gd_bT^2} \qquad \text{(assuming shallow water)} \tag{8}$$

The preliminary (linear) gradient of the profile is evaluated at closure depth, d_c, (the outer root of the transport polynomial) from Dean (1977) and Kriebel et al (1991):

$$\tan\beta = \left(\frac{2.25}{d_c}\left(\frac{w^2}{g}\right)^{\frac{1}{3}}\right)^{\frac{3}{2}} x_c^{-1} \qquad \text{Where } x_c \text{ is the offshore distance to closure.} \tag{9}$$

The model starts at high tide with a vertical increment of 0.1 metres. Water depth is simply calculated by subtracting the profile level (initially linear) from the still water level. Next a simple model of shoaling wave height is used to determine velocity scales to apply to the polynomial coefficients. The model, again using shallow water approximations is linear from the shore to the breakpoint (depth = 0:gd), and offshore of the breakpoint, takes the form

$$H = \left(\frac{d_b}{d}\right)^{\frac{1}{4}} H_b \tag{10}$$

The shoaling wave heights are used to calculate cross-shore varying maximum orbital velocities from:

$$u_{max} = \frac{H}{2}\sqrt{\frac{g}{d}} \tag{11}$$

u_{max} is used to evaluate $\overline{u^2}$ by assuming a sinusoidal variation in u within the wave period. $\overline{u^2}$ is then used to scale the transport coefficients. Normalised depth, i.e. depth over breaking depth, is calculated cross-shore, so that bedload and suspended load velocity terms may be calculated from the B-BAND derived coefficients giving the $u^2|u|$ term for bedload transport and $u^3|u|$ for suspended load transport. The transport coefficients from the B-Band field data are then:

$$Ibed_{coeff} = \frac{\overline{u^2|u|}}{\left(\overline{u^2}\right)^{3/2}}\left\{-1.58\left(\frac{d}{d_c}\right)^3 + 5.79\left(\frac{d}{d_c}\right)^2 - 4.59\left(\frac{d}{d_c}\right)\right\} \quad \text{bed load} \tag{12}$$

$$Isus_{coeff} = \frac{|u^3|u}{\left(\overline{u^2}\right)^2}\left\{-4.15\left(\frac{d}{d_c}\right)^3 + 14.17\left(\frac{d}{d_c}\right)^2 - 10.48\left(\frac{d}{d_c}\right)\right\} \quad \text{suspended load} \tag{13}$$

The expression for bed and suspended load transport, i, from Bagnold (1966) and Bowen (1980) is:

$$\dot{i}_{bed} = \frac{\varepsilon_b C_D \rho Ibed_{coeff}}{\tan\phi - \frac{u\beta}{|u|}} \tag{14}$$

$$\dot{i}_{suspended} = \frac{\varepsilon_s C_D \rho Isus_{coeff}}{W - u\beta} \tag{15}$$

where ε_b is a bedload efficiency factor, C_d is the drag coefficient for the bed, ρ the density of fluid, $\tan\phi$ is the angle of repose of sediment and $\tan\beta$ the beach slope. Similarly for suspended load transport ε_s is a suspended load efficiency factor, w is the sediment fall velocity and u is the instantaneous orbital velocity. Because our data provides a time averaged expression for $u^2|u|$ and $u^3|u|$ respectively, it is difficult to isolate the instantaneous orbital velocity to evaluate the slope terms in the denominator of the two expressions. In this contribution they are ignored (ie. $u\beta$ is set to zero in the denominators).

The total cross-shore immersed weight sediment transport rate is the sum of expressions (14) and (15), and the total volumetric transport rate, Q, is thus determined by:

$$Q = \frac{i_{bed} + i_{suspended}}{(\rho_s - \rho_w)g(1-n)} \tag{16}$$

where ρ_s and ρ_w are the sediment and fluid densities, g is gravity and (1-n) is the packing of settled grains (where n is the void ratio).

The sediment is then moved across the profile on the basis of the gradient of the volumetric transport rate, and the submerged part of the new profile is smoothed so that each point on the new profile is elevated or lowered to the mean of the height of its two neighbours. Having completed all these calculations for a particular tide level, the tide is moved at intervals of 1/100th of a tidal cycle through a simple sinusoid, and the process repeated.

Clearly the model works on several underlying assumptions, which may be summarised as follows:

1. The energetics model is valid.
2. Downslope and upslope transport are equal.
3. Airy wave theory is appropriate.
4. There is transmission of wave energy through bars.
5. Longshore transport is ignored.
6. Swash zone transport is ignored.
7. Sediment supply is unlimited.
8. No avalanching can occur.
9. There is a sinusoidal monochromatic tide signal.

Model Results and Discussion

Figure 4(a) shows the results of a model run with zero tidal range and a 2m breaking wave. Sediment is continually eroded at the shoreline and deposited offshore. The transport convergence point gradually moves offshore, the rate of movement being governed by the asymmetry of the transport profile in the surf zone, and the magnitude and asymmetry of the transport profile in the shoaling wave zone. As the profile evolves what started initially as an area of onshore erosion in the shoaling wave zone gets filled in by the offshore movement of sediment due to broadening of the surf zone. The plateau corresponds to the level of peak offshore transport, as modified by the wave energy profile. The onshore transport region quickly narrows into a spike as the beach gradient in the shoaling zone becomes steeper and steeper. Profile changes from cycle to cycle get smaller, suggesting that the model is approaching an equilibrium state.

Figure 4(b) shows what happens in the model when a tide range is introduced, so that the water surface is continually fluctuating and the transport zones migrate up and down the beachface. A pronounced high water bar forms, but

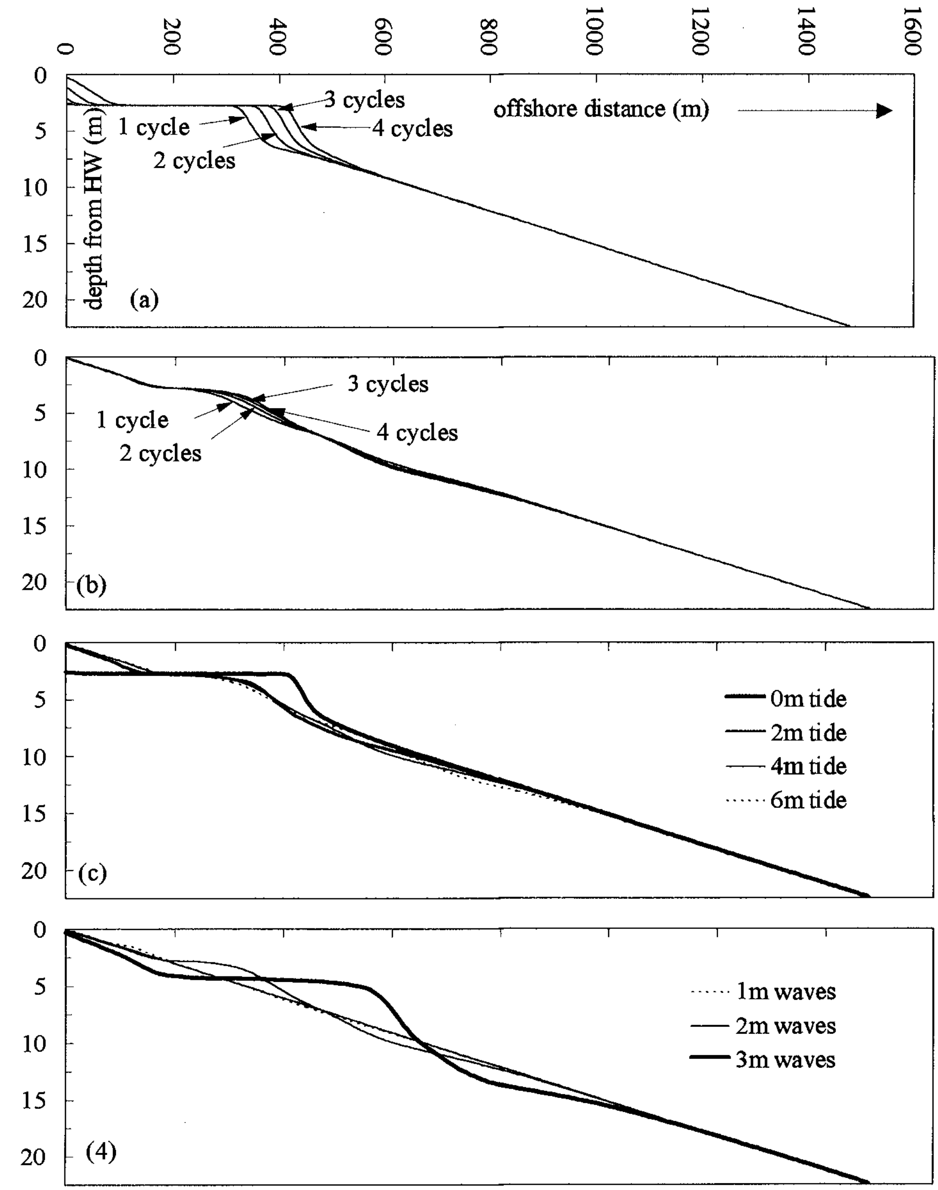

Figure 4. (a) Profile evolution through four tidal cycles with no tidal range and 2m wave height. (b) With 4m tidal range and 2m wave height. (c) Model sensitivity to tidal range 2, 4 and 6m tides (all with 2m waves). (d) Model sensitivity to wave height: 1, 2 and 3m breaking waves (all with 4m tide range).

the low water bar, corresponding to a depth from high water of approximately 6 metres, appears to be suppressed as a result of residence in both offshore and onshore transport zones. The area shoreward of the high water bar only ever resides in a zone of offshore erosion. Again the pattern of erosion and deposition is determined by the total effect of the transport profile, as modified by the shoaling wave energy profile. As the profile develops it appears to be approaching an equilibrium, and changes through time become progressively smaller. Because of the smoothing technique used, what is happening at the shoreline and in the offshore regions is that the elevation of cells outside of the transport zone is being modified by those inside, simulating a slumping effect. This model will only run for approximately 4 tidal cycles before it demands sediment from the very top, or very bottom of the profile, and fails a volume eontinuity test.

Figure 4(c) shows the evolution of the model profile under different tidal regimes after 4 tidal cycles, with 2 metre waves. The figure demonstrates the suppressing effect of larger tide ranges, with morphological change being the least for the 6m tidal range. In addition with the 6m range the high and low water bars become separated from each other. The position of the high water bar is similar for all cases except for the case of no tide range, where the amount of erosion has pushed it slightly further offshore.

Figure 4(d) shows the sensitivity of the model to wave height, it can be seen that the effect of increasing the wave height is similar to a reduction in tidal range - an increase in the magnitude of wave height leads to tendency for the profile to resemble the non-tidal case. 1m waves have a negligible effect on the profile even after 4 tidal cycles, while with 3m waves the erosion is so substantial, that, as with the zero tide case, the bar is moved offshore by the erosion, to the extent that it becomes indistinct from onshore accretion at low water.

Conclusion

At this stage in its development the model is not able to *quantitatively* simulate the cross-shore profile evolution on 2-dimensional beaches from a knowledge of the wave and tide regimes and sediment characteristics, although that is a possibility with further development. What has been shown is that, using quantitatively accurate flux profiles, the model produces realistic beach profiles within reasonable time-scales. Also, as has been observed by researchers examining field data from macrotidal beach sites (e.g. Wright et al (1982), Jago & Hardisty (1984), Short (1991), Masselink (1993), Masselink and Short (1993)), the model is able to confirm that wave height and tide range are the key influences on the form of the cross-shore profile.

The qualitative appearance of realistic features (offshore bar, intertidal terrace) indicates that the scale of macrotidal beach profile features can be predicted by the tidal translation of a transport shape function across the beachface. The model will now be used to explore more complex scenarios such as profile response to tide & wave field variations, and examine the effect of spring/neap variations within the tidal cycle.

Acknowledgements

This work was supported through funding by the Environmental and Physical Sciences Research Council, research grant reference 94305086.

References

Allen, J.R.L. (1970), *Physical Processes of Sedimentation,* George Allen and Unwin, London.

Bagnold, R.A. (1963), Mechanics of marine sedimentation, In: *The Sea, Ideas and Observations*, Wiley-Interscience Publishers, New York, **3**, 507-528.

Bagnold, R.A. (1966), An approach to the sediment transport problem from general physics, *U.S. Geol. Surv. Prof. Paper* 422-1.

Bailard, J.A. (1981), An energetics total load sediment transport model for a plane sloping beach, *Journal of Geophysical Research* **86**, 10938-10954.

Bailard, J.A. (1987), Surfzone wave velocity moments, *Proceedings of Coastal Hydrodynamics, ASCE,* 328-342.

Bird, A.C.F. (1969), *Coasts,* Australian National University Press, Canberra.

Bowen, A.J. (1980), Simple models of nearshore sedimentation; beach profiles and longshore bars, In: *The Coastline of Canada*, Ed. S.B. McCann, Geological Society of Canada, Paper 1-11.

Davidson, M.A., Russell, P.E., Huntley, D.A. and Hardisty, J. (1993), Tidal asymmetry in suspended sand transport on a macrotidal intermediate beach, *Marine Geology* **110**, 333-353.

Dean, R.G. (1977), Equilibrium beach profiles: U.S. Atlantic and Gulf coasts, *Ocean Engineering Technical Report #12*, 45pp.

Foote, Y.L.M. (1994), Waves, Currents and Sand Transport Predictors on a Macro-Tidal Beach, *Ph.D. Thesis.* Institute of Marine Studies, University of Plymouth.

Foote, Y.L.M., Huntley, D.A. and O'Hare, T.J. (1994), Sand transport on macro-tidal beaches, *Proceedings of the Euromech 310 colloquium*, Le Havre, 360-374.

Galvin, C.J. (1972), Waves breaking in shallow water, In: *Waves on Beaches*, Ed. R. Meyer, Academic Press, London, 413-455.

Guza, R.B. and Thornton, E.B. (1985), Velocity moments in the nearshore zone, *Journal of Waterways, Port, Coastal and Ocean Engineering*, **111**, 235-256.

Jago, C.F. and Hardisty, J. (1984), Sedimentology and morphodynamics of a macrotidal beach, Pendine Sands, SW Wales, *Marine Geology* **60**, 123-154.

Kriebel, D.L., Kraus, N.C. and Larson, M. (1991), Engineering methods for predicting beach profile response, *Proceedings of Coastal Sediments '91*, 557-571.

Le Mehaute, B. (1961), A theoretical study of waves breaking at an angle with a shoreline, *Journal of Geophysical Research* **66** no.2, 495-499.

Masselink, G. (1993), Simulating the effects of tides on beach morphodynamics, *Journal of Coastal Research* **15**, 180-197.

Masselink, G. and Short, A.D. (1993), The effect of tide range on beach morphodynamics and morphology: a conceptual model, *Journal of Coastal Research* **93**, 785-800.

O'Hare, T.J. (1994), What is the origin of the macro-tidal beach profile? *Unpublished Report,* Institute of Marine Studies, University of Plymouth.

Russell, P.R. and Huntley, D.A., (1996), The spatial distribution of cross-shore transport on high energy beaches, *(in prep.)* Institute of Marine Studies, University of Plymouth.

Short, A.D. (1991), Macro-meso tidal beach morphodynamics - an overview, *Journal of Coastal Research* **72**, 417-436.

U.S. Army Corps of Engineers, CERC (1984), *Shore Protection Manual*, 4th Ed, (2 vols), U.S. Printing Office, Washington DC.

Wright, L.D., Nielsen, P., Short, A.D. and Green, M.O. (1982), Morphodynamics of a macrotidal beach, *Marine Geology* **50**, 97-128.

Wright, L.D. and Short, A.D. (1984), Morphodynamic variability of surf zones and beaches: a synthesis, *Marine Geology* **56**, 93-11.